molecular pharmaceutics

pubs.acs.org/molecularpharmaceutics

Article

Improved Liver Delivery of Primaquine by Phospholipid-Free Small Unilamellar Vesicles with Reduced Hemolytic Toxicity

Nojoud AL Fayez, Roland Böttger, Elham Rouhollahi, Pieter R. Cullis, Dominik Witzigmann, and Shyh-Dar Li*

Cite This: *Mol. Pharmaceutics* 2022, 19, 1778−1785

Read Online

ACCESS | Metrics & More | Article Recommendations | Supporting Information

ABSTRACT: Hemolytic toxicity caused by primaquine (PQ) is a high-risk condition that hampers the wide use of PQ to treat liver-stage malaria. This study demonstrated that phospholipid-free small unilamellar vesicles (PFSUVs) composed of Tween80 and cholesterol could encapsulate and deliver PQ to the hepatocytes with reduced exposure to the red blood cells (RBCs). Nonionic surfactant (Tween80) and cholesterol-forming SUVs with a mean diameter of 50 nm were fabricated for delivering PQ. Drug release/retention, drug uptake by RBCs, pharmacokinetics, and liver uptake of PFSUVs-PQ were evaluated in *in vitro* and *in vivo* models in comparison to free drugs. Additionally, the stress effect on RBCs induced by free PQ and PFSUVs-PQ was evaluated by examining RBC morphology. PFSUVs provided >95% encapsulation efficiency for PQ at a drug-to-lipid ratio of 1:20 (w/w) and stably retained the drug in the presence of serum. When incubated with RBCs, PQ uptake in the PFSUVs group was reduced by 4- to 8-folds compared to free PQ. As a result, free PQ induced significant RBC morphology changes, while PFSUVs-PQ showed no such adverse effect. Intravenously (i.v.) delivered PFSUVs-PQ produced a comparable plasma profile as free PQ, given i.v. and orally, while the liver uptake was increased by 4.8 and 1.6-folds, respectively, in mice. Within the liver, PFSUVs selectively targeted the hepatocytes, with no significant blood or liver toxicity in mice. PFSUVs effectively targeted PQ to the liver and reduced RBC uptake compared to free PQ, leading to reduced RBC toxicity. PFSUVs exhibited potential in improving the efficacy of PQ for treating liver-stage malaria.

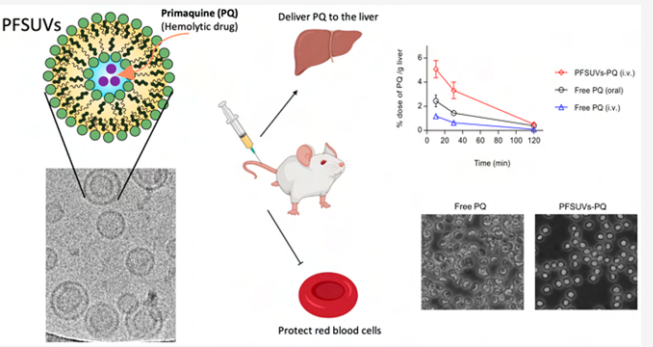

KEYWORDS: *phospholipid-free small unilamellar vesicles (PFSUVs), primaquine (PQ), red blood cells (RBCs), liver targeting, liver-stage malaria*

INTRODUCTION

Malaria remains one of the most lethal parasitic diseases in tropical regions around the world. According to the World Health Organization (WHO), there are more than 200 million new cases of malaria annually.[1] Malaria is mainly transmitted to humans by mosquito bites, and then the sporozoites are carried through the blood to the liver. In humans, *Plasmodium vivax*, *P. ovale*, *P. falciparum*, and *P. malariae* are the common four species of parasites responsible for the malaria infection. When sporozoites reach the liver, they infiltrate the hepatocytes, replicate, and finally cause rupture of the hepatocytes, releasing merozoites that can penetrate the red blood cells (RBCs). The parasites then continue their asexual blood stage and eventually burst the host RBCs, presenting clinical symptoms.[2] Notably, the parasites can be dormant in the liver and cause malaria relapse weeks or even years after infections.[3] Most antimalarial drugs, such as chloroquine, hydroxychloroquine, and mefloquine, are only effective in the blood stage, while 8-aminoquinolines, including primaquine (PQ) and tafenoquine (TQ), are also effective for the hepatic stage of *P. vivax* and *P. ovale*, with potential to cure malaria.[4] However, the wide use of PQ and TQ for malaria therapy has been limited as they both induce significant hemolytic toxicity, particularly in individuals with glucose-6-phosphate dehydrogenase deficiency (G6PDd).[5,6] Patients with G6PDd have limited ability to regenerate nicotinamide adenine dinucleotide phosphate (NADPH) and glutathione (GSH) in their erythrocytes, resulting in increased oxidative stress levels and eventually hemolytic anemia when treated with either PQ or TQ.[7,8]

We hypothesized that a drug delivery system that can stably encapsulate PQ/TQ during the blood circulation and target

Special Issue: Tiny Things, Huge Impact: Nanomedicine in Canada

Received: June 29, 2021
Revised: September 12, 2021
Accepted: September 13, 2021
Published: September 21, 2021

the hepatocytes will reduce the drug exposure to the RBCs and increase the drug targeting to the liver, leading to improved therapy of liver-stage malaria. In previous publications, we have described the development of PFSUVs (phospholipid-free small unilamellar vesicles), an innovative delivery system, showing significant accumulation in the hepatocytes, where the malaria parasites reside. This delivery system is composed of cholesterol and Tween80, hence the name "phospholipid-free" to differentiate from standard liposomal SUVs that are made of phospholipids. Although there have been many different nanoparticles developed for drug delivery, the vast majority of them were captured by the Kupffer cells and eliminated.[9,12] Here, we report the utilization of this formulation for targeting PQ to the liver with reduced RBC exposure and toxicity. We fabricated the particles using microfluidics and optimized the active loading protocol for PQ with detailed characterizations of the final formulation. We then examined the ability of the particles to stably retain PQ in the presence of serum and compared their RBC uptake and toxicity with free PQ. Finally, pharmacokinetics and liver uptake of free PQ and PQ loaded in the particles were evaluated and compared in mice. The safety of this nanoparticle formulation was also studied in mice by examining the blood chemistry and liver histology.

MATERIALS AND METHODS

Chemical and Reagents. Human red blood cells (RBCs) were purchased from Innovative Research (Novi, MI). Dialysis membrane (10 kDa molecular weight cutoff, MWCO) was purchased from Spectrum Laboratories (Waltham, MA). All other organic solvents, reagents, and buffers were of analytical grade and obtained from Sigma-Aldrich (Oakville, ON, Canada).

PFSUVs Preparation and Characterization. PFSUVs with a cholesterol (Chol)/Tween80 molar ratio of 5:1 were prepared as previously described.[9] Briefly, the formulation was fabricated using a microfluidic mixing system (NanoAssemblr Benchtop, Precision Nanosystems, Vancouver, BC, Canada). Chol and Tween80 were dissolved in ethanol at a final concentration of 10 mg/mL and mixed with 250 mM ammonium sulfate in the microfluidic system at a flow ratio of 1:3. Particles were produced at a total flow rate of 15 mL/min at room temperature and dialyzed against HEPES (4-(2-hydroxyethyl)-1-piperazineethanesulfonic acid) buffered saline (HBS, pH 7.4) overnight to remove ethanol. PFSUVs were then concentrated using a tangential flow filtration (TFF) system (KrosFlo KR2i, Spectrum Laboratories, Rancho Dominguez, CA) operating in the ultrafiltration mode and filtered through a diafiltration cartridge with an MWCO of 500 kDa (MidiKros Hollow Fiber Filter, surface area = 115 cm^2, fiber inner diameter = 0.5 mm, length = 20 cm, Spectrum Laboratories) at a flow rate of 40 mL/min and concentrated to 25 mg lipid/mL. The average particle size and polydispersity index were measured by dynamic light scattering (DLS) using Zetasizer NanoZS (Malvern Instruments, Malvern, UK). For fluorescent-labeled PFSUVs, DiR (lipophilic carbocyanine DiOC18(7) dye) was added to the lipid solution at 1.1 mol % followed by the same preparation process.

PQ Loading into PFSUVs. PQ was loaded into PFSUVs (25 mg/mL total lipids) by the active loading method. Briefly, PFSUVs were mixed with PQ at various drug-to-lipid (D/L) ratios ranging from 1:20 to 1:5 (w/w). The mixture was incubated for 1 h at 37 °C and then quenched on ice for 2 min. The formulation was then dialyzed against HBS overnight. The encapsulation efficiency (EE) was determined using ultra performance liquid chromatography (UPLC) by comparing the D/L before and after dialysis. For UPLC analysis, 15 μL of PFSUVs was mixed with 45 μL of ethanol and sonicated for 5 min, followed by injection of 10 μL of the sample.

Ultra Performance Liquid Chromatography (UPLC). PQ concentration was analyzed using an ACQUITY UPLC H-Class System (Waters, Milford, MA) coupled online to a photodiode array (PDA) detector (wavelength = 265 nm) and a QDa mass spectrometer operated in positive ionization mode. For mass spectrometry, the ionization was carried out at 250 °C (source temperature) using a cone voltage of 65 V, and the concentration of PQ was determined by integrating the single ion recognition (SIR) peak for the singly charged molecular ion (m/z 260.1) acquired at a capillary voltage of 0.5 V. Tween80 and Chol concentrations were also analyzed using the same chromatography system coupled to an evaporative light scattering (ELS) detector. Separation relied on a BEH-C18 column (inner diameter = 2.1 mm; length = 100 mm; particle size = 1.7 μm, Waters) at a flow rate of 0.3 mL/min using a gradient mobile phase containing a mixture of eluents A and B (0.1% v/v aqueous TFA and 0.1% v/v TFA in methanol, respectively). The following gradient was employed: 0 min: A/B (95:5); 2 min: A/B (95:5); 8 min: A/B (0:100); 11 min: A/B (0:100); 11.1 min: A/B (95:5); 13 min: A/B (95:5).

Cryogenic Transmission Electron Microscopy (Cryo-oTEM). PFSUVs and PFSUVs-PQ (25 mg lipid/mL) were deposited onto a glow-discharged copper grid, vitrified using an FEI Mark IV Vitrobot (FEI, Hillsboro, OR), and imaged using a 200 kV Glacios microscope equipped with a Falcon III camera at the UBC High Resolution Macromolecular Cryo-Electron Microscopy facility (Vancouver, BC).

***In Vitro* Drug Retention.** PFSUVs-PQ (~1.2 mg PQ/mL) was mixed with either HBS or fetal bovine serum (FBS) (Gibco Laboratories, Gaithersburg, MD) at a 1:1 ratio (v/v) and incubated at 37 °C. After 10, 30, and 120 min, 200 μL of the sample was collected and purified by size exclusion chromatography (SEC) on a Sephacryl packed gel to remove the leaked drug. Forty-five μL of the sample before and after SEC was mixed with 300 μL of ethanol, and the mixture was vortexed for 30 s, placed on ice for 30 min, and centrifuged twice at 12 500 rpm for 5 min. The supernatant (280 μL) was collected, lyophilized, and reconstituted in 45 μL of ethanol. Ten μL of the sample was then injected into the UPLC for PQ, Tween80, and Chol analysis as described above. Drug retention was calculated following eq 1, where $(D/L)_i$ and $(D/L)_f$ are the initial and final drug-to-lipid ratios, respectively.

$$\text{drug retention} = \left(1 - \frac{(D/L)_i - (D/L)_f}{(D/L)_i}\right) \times 100 \quad (1)$$

RBC Uptake of PQ. Human RBCs were washed with phosphate buffered saline (PBS) twice and resuspended in PBS at a final hematocrit of 5%. RBCs were incubated at 37 °C with either PFSUVs-PQ or free PQ at concentrations of 0.05−0.16 mg PQ/mL for 10 min. This range of concentrations was estimated to include C_0 in our *in vivo* pharmacokinetic study (see below). RBCs were then collected by centrifugation at 3000 rpm for 5 min, lysed with 1 mL of lysis buffer (BD Biosciences, San Jose, CA) at room temperature for 15 min, and centrifuged at 3000 rpm for 5 min. Forty-five μL of the

https://doi.org/10.1021/acs.molpharmaceut.1c00520
Mol. Pharmaceutics 2022, 19, 1778−1785

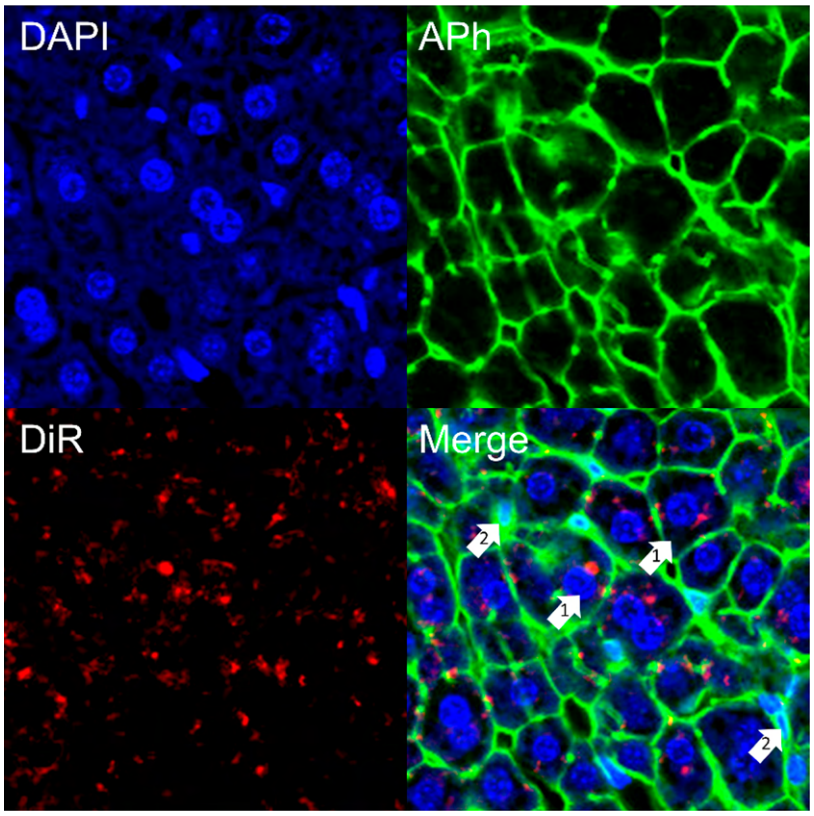

Figure 1. Intraliver distribution of DiR-labeled PFSUVs. Confocal microscopy images of liver sections collected from female CD-1 mice 2 h after injection with DiR-labeled PFSUVs (red). Sections were stained with DAPI (blue) and Alexa Fluor 488 Phalloidin (green). Arrows 1 and arrows 2 represent hepatocytes and Kupffer cells, respectively, identified by their nuclear morphology and phalloidin staining.

supernatant was collected, processed, and analyzed by UPLC as described in the drug retention study.

Erythrocytes Morphology. The experimental protocol was adopted from a previous report.[10] Human RBCs were diluted to a final hematocrit of 2% and incubated with either saline, free PQ, or PFSUVs-PQ at 0.5 mg PQ/mL at 37 °C for 10 min. Ten μL of the sample was placed on a glass slide for imaging by a light-inverted microscope utilizing a 40× magnification objective (Olympus CKX41, Tokyo, Japan).

***In Vitro* Hemolysis.** Human RBCs (2% hematocrit) were incubated with free PQ or PFSUVs-PQ at a range of concentrations (0.025, 0.05, and 0.1 mg PQ/mL) at 37 °C for 2 h and centrifuged at 5000*g* for 10 min at 4 °C. The supernatant was collected and measured for the absorbance at 540 nm using a microplate reader. PBS and 10% Triton-X 100 in water (w/v) were used as the negative and positive control, respectively. The relative hemolysis (RH) was calculated using eq 2:

$$\mathrm{RH}\% = \frac{R_s - R_n}{R_p - R_n} \quad (2)$$

where R_s, R_n, and R_p are the absorbance of the sample, negative control, and positive control, respectively.

Animals. Female CD1 mice (18−20 g, 6−7 weeks old) were purchased from The Jackson Laboratory (Bar Harbor, ME). All *in vivo* studies were conducted in accordance with an established protocol approved by the Animal Care Committee of the University of British Columbia (Vancouver, BC, Canada).

Intrahepatic Distribution. Mice were i.v. injected with PFSUVs-DiR at a dosage of 0.3 μg DiR/g. Two hours post injection, mice were sacrificed, and the liver was harvested immediately, followed by washing with PBS and storage in 10% (v/v) formalin in PBS overnight at room temperature. Tissue sections with a thickness of 40 μm were prepared from the formalin-fixed livers using a vibratome (Precisionary Instruments LLC, Boston, MA). Sections were collected in PBS and subsequently incubated in 0.1% (v/v) Triton X-100 in PBS for 5 min, washed with PBS three times, and then incubated in 1% (v/v) bovine serum albumin in PBS for 10 min. Sections were washed 3 times with PBS then incubated in Alexa Fluor 488 Phalloidin (APh, 80 μL, 1 U/mL). Finally, sections were further washed with PBS to remove excess staining and mounted on a glass slide with a drop of Fluoroshield containing DAPI (Sigma-Aldrich). The stained section was imaged using a confocal microscope (Zeiss LSM 700) at 20× magnification and analyzed with ZEN software (both Carl Zeiss, Oberkochen, Germany).

Pharmacokinetics. PFSUVs-PQ dissolved in HBS was administered to mice via i.v. injection, and free PQ dissolved in saline was administered through either the tail-vein or oral gavage at 5 mg PQ/kg (100 mg lipid/kg). At 10, 30, and 120 min, blood was collected and was quickly transferred into an EDTA-coated tube. Plasma was isolated by centrifugation at 4 °C for 10 min at 500*g*. Forty-five μL of plasma was then processed and analyzed for PQ following the same UPLC protocol as described above. After animal euthanasia, a piece of liver (~0.2 g) was excised and washed twice with PBS, blotted dry, and weighed into a 1.5 mL microtube (Next Advance, Inc., Troy, NY). PBS containing the protease inhibitor cocktail

https://doi.org/10.1021/acs.molpharmaceut.1c00520
Mol. Pharmaceutics 2022, 19, 1778−1785

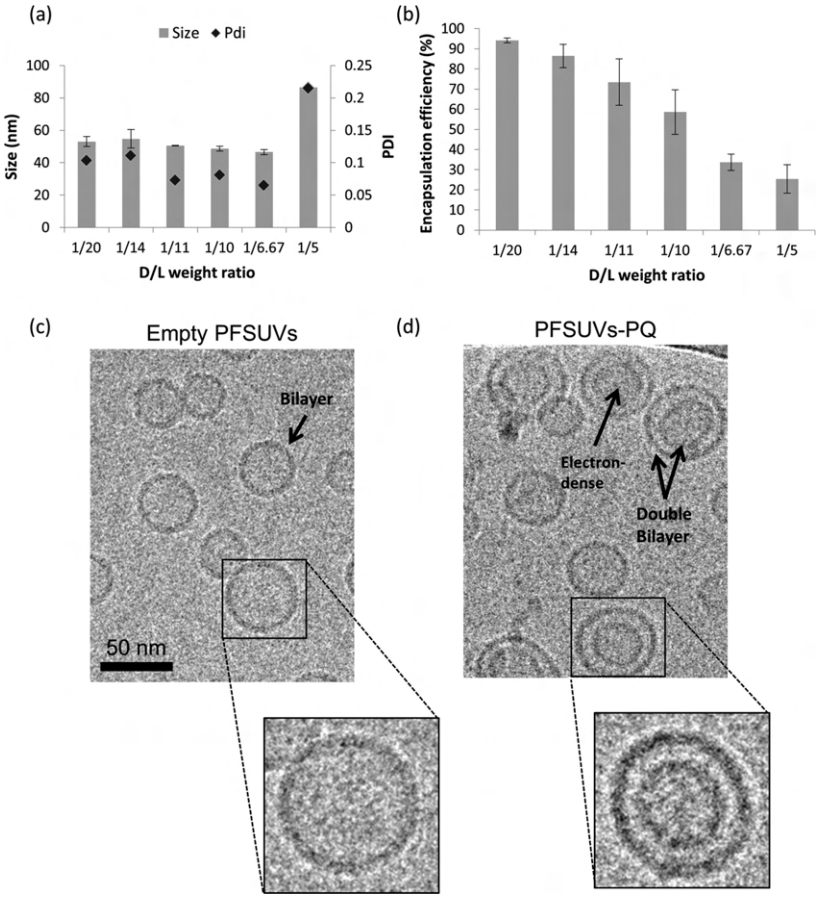

Figure 2. Characterization of PFSUVs-PQ. (a) Particle size and PDI of PFSUVs-PQ prepared with different D/L ratios. Data = mean ± SD (n = 3). (b) Drug encapsulation efficiency of PFSUVs prepared with different D/L ratios. Data = mean ± SD (n = 3). (c, d) Cryo-TEM images of empty PFSUVs and PFSUVs-PQ.

(1:100 v/v dilution, Sigma-Aldrich) was added (0.3 mL per 0.1 g tissue), and tissue homogenization was performed with a tissue homogenizer Bullet blender (Next Advance, Inc., Troy, NY) at an instrument speed of 10 for 5 min at 4 °C. The homogenate (45 μL) was then processed using the same protocol described above for UPLC analysis of PQ.

Toxicology of PFSUVs in Mice. Mice were injected i.v. with empty PFSUVs at 100 mg of total lipid/kg (equivalent to 5 mg PQ/kg). Blood was collected from the mice 24 h post injection, followed by euthanasia. Whole blood (0.5 mL) was collected in an EDTA Minicollect tube (Greiner Bio-one, Kremsmünster, Austria) and stored at 4 °C. Serum was obtained by collecting 0.3 mL of blood in a clot activator tube (Microvette, Sarstedt AG & Co., Nümbrecht, Germany) incubated for 20 min at room temperature, followed by centrifugation at 10 000g for 5 min. Complete blood count (CBC) and serum alanine aminotransferase (ALT) and aspartate aminotransferase (AST) were measured by IDEXX Reference Laboratories Ltd. (Delta, BC, Canada) and compared to the reference values provided by Charles River. The liver was collected immediately after euthanasia, washed with PBS, and stored in 10% (v/v) formalin in PBS for 48 h at room temperature. Paraffin-embedded liver section, hematoxylin and eosin staining, and microscopic imaging were performed by Wax-it Histology Services Inc. (Vancouver, BC, Canada).

Statistical Analysis. All data are presented as mean ± SD. Statistical analysis was performed with GraphPad Prism version 8.0 (GraphPad Software, San Diego, CA). Comparisons between groups were made by one-way ANOVA. A difference with $p < 0.05$ was considered to be statistically significant.

RESULTS AND DISCUSSION

Preparation and Optimization of PQ Loaded PFSUVs. While many drugs are effective for the blood stage of malaria, such as chloroquine and mefloquine, only PQ and TQ are active against the liver stage of the disease. However, both PQ and TQ generate oxidative stress within erythrocytes, causing hemolysis, which is particularly severe in patients with G6PD enzyme deficiency.[11] This limits the wide use of PQ and TQ for the therapy of malaria. The project was aimed at developing a delivery system that could reduce RBC uptake of PQ and target PQ to the hepatocytes, thus reducing the toxicity and improving the efficacy against liver-stage malaria.

We have previously developed a lipid-based nanoparticle formulation, named PFSUVs, that can stably retain weak base drugs in the serum and effectively deliver to the hepatocytes after i.v. delivery.[9] Our data showed that PFSUVs fabricated using the staggered herringbone mixer (SHM) microfluidic system with a 5:1 molar ratio of Chol/Tween80 displayed predominant accumulation in the liver.[12] In this study, we further demonstrated that within the liver, PFSUVs selectively accumulated in the hepatocytes as soon as 2 h post injection. As shown in Figure 1, the hepatocytes (indicated by arrow 1) can be identified through the phalloidin staining and their

https://doi.org/10.1021/acs.molpharmaceut.1c00520
Mol. Pharmaceutics 2022, 19, 1778−1785

distinct nuclear morphology from the Kupffer cells (indicated by arrow 2), and approximately ~70% of DiR-labeled PFSUVs were detected within the hepatocytes. This would make PFSUVs a suitable delivery system for PQ to improve the treatment of liver-stage malaria. In the following, we explored using PFSUVs for targeted delivery of PQ to the liver, while reducing the uptake by the RBCs, with a goal to resolve the challenges of PQ for treating malaria.

To encapsulate PQ into PFSUVs, Chol and Tween80 were dissolved in ethanol and then rapidly mixed with 250 mM ammonium sulfate in a microfluidic chip. As the lipid solution mixed with the aqueous phase, Chol and Tween80 self-assembled into SUVs due to the increase in polarity. After ethanol removal via dialysis and concentration through the TFF system, PFSUVs containing an ammonium sulfate gradient were produced with a mean diameter of 50 ± 3.45 nm, a polydispersity index (PDI) of 0.10 ± 0.05, and a neutral ζ potential of −0.29 ± 0.38 mV. PQ was then actively loaded into PFSUVs by incubating PQ with PFSUVs at a range of drug-to-lipid (D/L) ratios (1:20 to 1:5) at 37 °C for 1 h. The formulations were then purified by dialysis against HBS and analyzed for their size, PDI, and drug encapsulation efficiency (EE). As shown in Figure 2a, the particle size and PDI remained constant at ~50 nm and ~0.1, respectively, for all preparations except for that with a high D/L of 1:5 exhibiting an increased mean size of ~80 nm and an increased PDI of >0.2 due to additional drug that could lead to a larger particle size by unstable incorporation into the bilayer. Additionally, the EE of PFSUVs prepared with a D/L of 1:20 was the highest at 95%, and the EE decreased with increasing D/L, suggesting the PQ loading capacity reached the maximum at a D/L of 1:20 (Figure 2b and Table 1). We then selected the formulation prepared with a D/L of 1:20 for the following studies.

Table 1. Characterization of PFSUVs-PQ Prepared with Different D/L Ratios[a]

D/L ratio (w/w)	size (nm)	PDI	encapsulation efficiency (%)	ζ potential (mV)
1:20	53.1 ± 3.1	0.10 ± 0.05	94.2 ± 1.2	−0.29 ± 0.38
1:14.3	54.7 ± 5.7	0.11 ± 0.03	86.6 ± 5.8	−1.21 ± 0.29
1:11.1	50.6 ± 0.8	0.07 ± 0.01	73.5 ± 11.5	−1.26 ± 0.56
1:10	48.7 ± 1.6	0.08 ± 0.01	58.6 ± 11.0	−0.66 ± 1.61
1:6.7	46.6 ± 1.6	0.06 ± 0.002	33.7 ± 4.1	−1.41 ± 0.91
1:5	86.6 ± 6.2	0.21 ± 0.06	25.4 ± 7.0	−0.14 ± 0.64

[a]Data = mean ± SD (n = 3).

Morphological characteristics (size, lamellarity, drug loading) of empty PFSUVs and PFSUVs loaded with PQ were analyzed using CryoTEM (Figure 2c,d). The PFSUV particles displayed a spherical shape with sizes between 50 and 60 nm, which was consistent with the DLS results. Relative to empty PFSUVs, the majority of the PFSUVs-PQ showed a double bilayer structure with an electron-dense structure inside the vesicles, suggesting PQ loaded inside the particle core.

Drug Retention. Drug retention in PFSUVs in the presence of serum is crucial for drug targeting. If PQ was burst-released from PFSUVs in serum, then PFSUVs-PQ would behave like free PQ after i.v. administration. Therefore, an *in vitro* drug release study was conducted to evaluate the ability of PFSUVs to retain PQ within the delivery system in the blood circulation until uptake by the liver. The optimized PFSUVs-PQ with a D/L of 1:20 was incubated with HBS or FBS at 1:1 (v/v) at 37 °C, and 10−120 min later, the sample was purified by size exclusion chromatography (SEC) to remove released PQ from PFSUVs-PQ. The concentration of PQ within PFSUVs was measured using UPLC (Figure 3). We

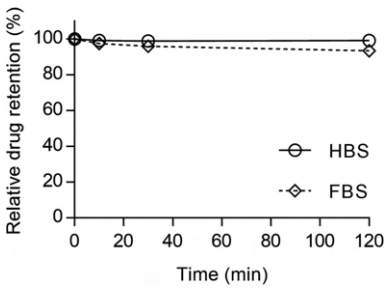

Figure 3. *In vitro* drug retention of PFSUVs-PQ in HEPES-buffered saline (HBS) or fetal bovine serum (FBS) at 37 °C. Data = mean ± SD (n = 3).

observed stable PQ retention within PFSUVs for a period of 120 min, demonstrating <10% drug leakage in serum. We did not examine longer time points as the vast majority of PFSUVs accumulated in the liver within 2 h after i.v. delivery.[9]

RBC Uptake of PQ. It has been shown that reactive oxygen species (ROS) induced by PQ causes hemolytic damage on RBCs,[5,6] and the RBC toxicity was found dependent on the drug concentration within the RBCs.[13] We hypothesized that free PQ would be readily accessible for RBCs through rapid diffusion, while loading PQ into PFSUVs would hinder the RBC uptake and reduce hemotoxicity. Here, we compared RBC uptake of free PQ and PFSUVs-PQ in an *in vitro* setting. We incubated free PQ or PFSUVs-PQ at concentrations of 0.05−0.16 mg PQ/mL with RBCs at 37 °C for 10 min. This range of concentrations was estimated to include C_0 in our *in vivo* pharmacokinetic study. RBCs were then collected and analyzed for PQ using UPLC-MS. As shown in Figure 4, free PQ displayed significantly increased RBC uptake compared to PFSUVs-PQ, with 8-fold and 4.3-fold increases at 0.05 mg PQ/mL and 0.16 mg PQ/mL, respectively.

***In Vitro* Hemolysis Assay.** Since PFSUVs exhibited the ability to rapidly accumulate in the liver and PFSUVs-PQ showed reduced RBC uptake, we hypothesized that PFSUVs-PQ would be less toxic to RBCs, inducing minimal hemolysis. We compared RBC toxicity of PQ and PFSUVs-PQ using hemolysis assay. As shown in Figure 5a, PFSUVs-PQ displayed

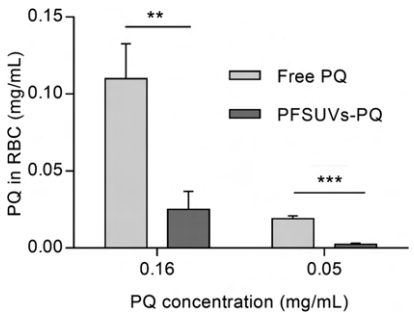

Figure 4. PQ concentrations in RBC after 10 min of incubation at 37 °C with free PQ or PFSUVs-PQ. Data = mean ± SD (n = 3). (*: P < 0.05; ****: P < 0.0001)

https://doi.org/10.1021/acs.molpharmaceut.1c00520
Mol. Pharmaceutics 2022, 19, 1778−1785

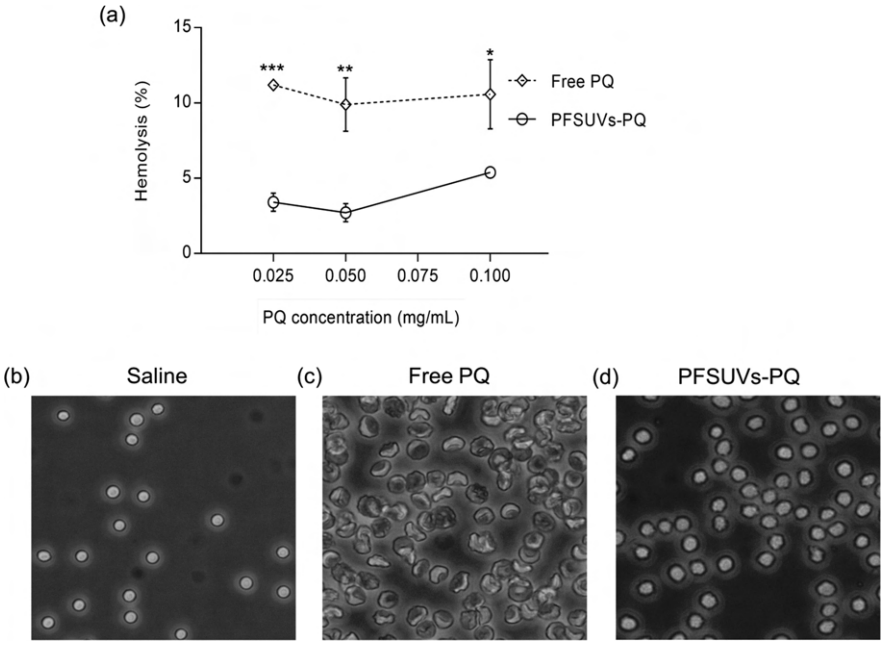

Figure 5. (a) Hemolysis of PFSUVs-PQ and free PQ after incubation with RBCs at 37 °C for 2 h. (b) RBCs morphology after incubation at 37 °C with saline, (c) free PQ, or (d) PFSUVs-PQ. (Data = mean ± SD (n = 3). (**: P < 0.001).

reduced hemolytic toxicity compared to free PQ at all of the tested concentrations including the calculated C_0 at 0.065 mg PQ/mL. It is noted that normal RBCs were used in this study due to lack of access to G6PDd samples, and therefore, the hemotoxicity was mild. Nevertheless, the results support that PFSUVs-PQ was significantly safer than free PQ.

Erythrocytes Morphology. The effect of PQ, as a stressor, on RBCs can also be displayed by a change in cell morphology,[14,15] and deformed RBCs will be removed by macrophages in the liver and spleen, leading to anemia. We incubated RBCs with PFSUVs-PQ or free PQ at 37 °C for 10 min and imaged the cells under light microscopy. A high concentration of 0.5 mg PQ/mL was used in this study to induce visible morphology change. As shown in Figure 5c, the RBC cell membrane deformed from a biconcave shape into a cup or bowl-like shape known as stomatocytes after incubation with free PQ.[16] However, when incubated with PBS (Figure 5b) or PFSUVs-PQ (Figure 5d), a little or no effect in membrane deformation was detected, suggesting increased safety with PFSUVs-PQ compared to free PQ. The results are consistent with the RBC uptake data.

***In Vivo* Pharmacokinetics.** The main goal of this research was to increase the delivery of PQ to the liver, while reducing its exposure to the RBCs. Thus, the efficacy of PQ against liver-stage malaria would be enhanced, and the RBC toxicity would be decreased. Pharmacokinetic studies in mice for free PQ and PFSUVs-PQ were preformed to compare the delivery of PQ in the plasma and liver. Free PQ or PFSUVs-PQ was i.v. injected into female CD-1 mice at a dose of 5 mg PQ/kg. Additionally, an oral dose of free PQ was administered and compared, since PQ is commonly given orally. The plasma and liver were collected at 10, 30, and 120 min post administration and analyzed for PQ. The plasma profiles of PQ for oral-PQ, i.v.-PQ, and PFSUVs-PQ are comparable as illustrated in Figure 6a and Table 2. However, the overall liver delivery by PFSUVs-PQ was increased by 4.5-fold and 2-fold compared to i.v.-PQ and oral-PQ, respectively, based on the area under the curve (AUC) comparison in Figure 6b. The AUC ratio between liver and plasma in the PFSUVs-PQ group was 4.8-fold and 1.6-fold higher than that in the i.v.-PQ and oral-PQ groups, respectively, indicating enhanced liver selectivity. Due

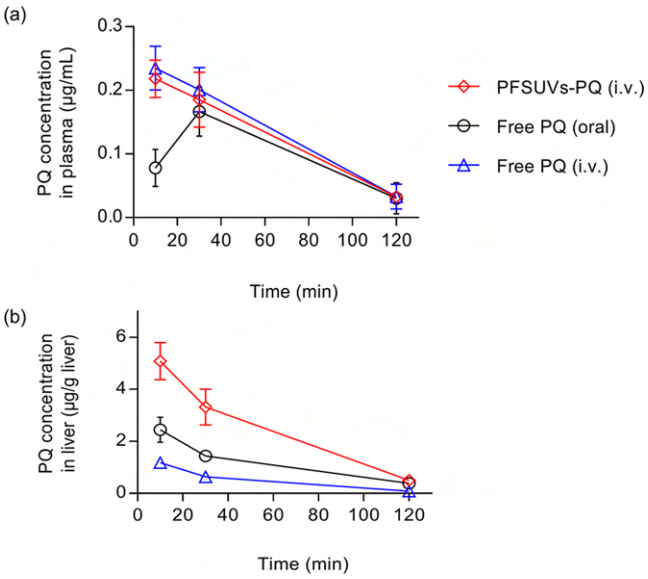

Figure 6. Pharmacokinetic profiles of i.v.-PFSUVs-PQ, i.v.-PQ, and oral-PQ in (a) plasma and (b) liver in female CD-1 mice after receiving a dose at 5 mg PQ/kg. Data = mean ± SD (n = 3−5).

Table 2. Area under the Curve Analysis of Pharmacokinetics Drug Profile (Figure 6)

	PFSUV−PQ (i.v.)	oral-PQ	i.v.-PQ
AUC_{plasma} (μg min/mL)	13.6 ± 3.2	11.2 ± 3.6	14.7 ± 3.1
AUC_{liver} (μg min/mL)	246.8 ± 49.3	125.6 ± 23.0	54.7 ± 11.9
AUC ratio (liver/plasma)	18.09	11.21	3.71

https://doi.org/10.1021/acs.molpharmaceut.1c00520
Mol. Pharmaceutics 2022, 19, 1778−1785

to the current lack of access to a disease model, further efficacy studies will be pursued in the future. However, together with the *in vitro* RBC data (Figures 4 and 5) and the PK results, our study suggested PFSUVs might improve efficacy against liver-stage malaria and reduce RBC toxicity of PQ.

***In Vivo* Toxicology Study of PFSUVs.** Finally, to examine the safety of PFSUVs as a delivery system, we i.v. injected empty PFSUVs at 100 mg lipid/kg (equivalent to 5 mg PQ/kg) into female CD-1 mice and collected blood and serum 24 h later, followed by euthanasia and liver harvest. Acute liver toxicity was evaluated by measuring ALT and AST and compared to the reference values provided by Charles River.[17] The acute effect of PFSUVs on the blood cells was determined by performing a complete blood count (CBC) analysis and compared to the reference values. As shown in Table 3, there was no significant change of the serum ALT, AST, and CBC panel after PFSUVs treatment, suggesting this delivery system was safe in an acute setting. The liver histology data also supported that PFSUVs were not toxic to the liver, although a large dose was delivered to the hepatocytes (Figure 7). These results indicate no significant acute toxicity of PFSUVs in mice. The safety of long-term use of PFSUVs will be studied in the future.

Table 3. Liver and Blood Toxicology Values Treated with Empty PFSUVs Compared to Normal Values

test	PFSUVs treated	normal
	Liver	
ALT (U/L)	39.33 ± 7.77	41.63 ± 13.91
AST (U/L)	75.00 ± 16.52	82.8 ± 39.85
	Blood	
RBC ($\times 10^{12}$/L)	8.05 ± 1.05	8.77 ± 1.12
hematocrit (L/L)	0.44 ± 0.05	0.49 ± 0.067
hemoglobin (g/L)	129.75 ± 13.91	145 ± 20.5
MCV (fL)[a]	54.05 ± 1.08	56.39 ± 3.75
MCH (pg)[a]	16.18 ± 0.61	16.59 ± 1.09
MCHC (g/L)[a]	298.85 ± 6.93	295.2 ± 26.5
RDW (%)[a]	16.83 ± 2.30	16.62 ± 1.09

[a]Abbreviations: MCV, mean corpuscular volume; MCH, mean corpuscular hemoglobin; MCHC, mean corpuscular hemoglobin concentration; RDW, red cell distribution width.

CONCLUSION

The current study demonstrated that PFSUVs composed of 83 mol % Chol and 17 mol % Tween80 were able to encapsulate PQ into the core of particles by active loading. PFSUVs stably retained PQ without significant drug leakage for 120 min in serum, reduced PQ uptake by the RBCs, and effectively targeted PQ to the liver compared to free PQ. Furthermore, PFSUVs effectively accumulated in the hepatocyte but displayed no acute blood or liver toxicity. The results showed the significant potential of using PFSUVs to improve the efficacy and safety of PQ for treating liver-stage malaria.

ASSOCIATED CONTENT

Supporting Information

The Supporting Information is available free of charge at https://pubs.acs.org/doi/10.1021/acs.molpharmaceut.1c00520.

DLS particle characterization, % dose/g liver of PQ in the liver in female CD-1 mice, and hematoxylin and eosin-stained sections of mouse liver (PDF)

AUTHOR INFORMATION

Corresponding Author

Shyh-Dar Li − *Faculty of Pharmaceutical Sciences, University of British Columbia, Vancouver, British Columbia V6T 1Z3, Canada; NanoMedicines Innovation Network (NMIN), University of British Columbia, Vancouver, British Columbia V6T 1Z3, Canada;* orcid.org/0000-0002-1763-2667; Email: shyh-dar.li@ubc.ca

Authors

Nojoud AL Fayez − *Faculty of Pharmaceutical Sciences, University of British Columbia, Vancouver, British Columbia V6T 1Z3, Canada*

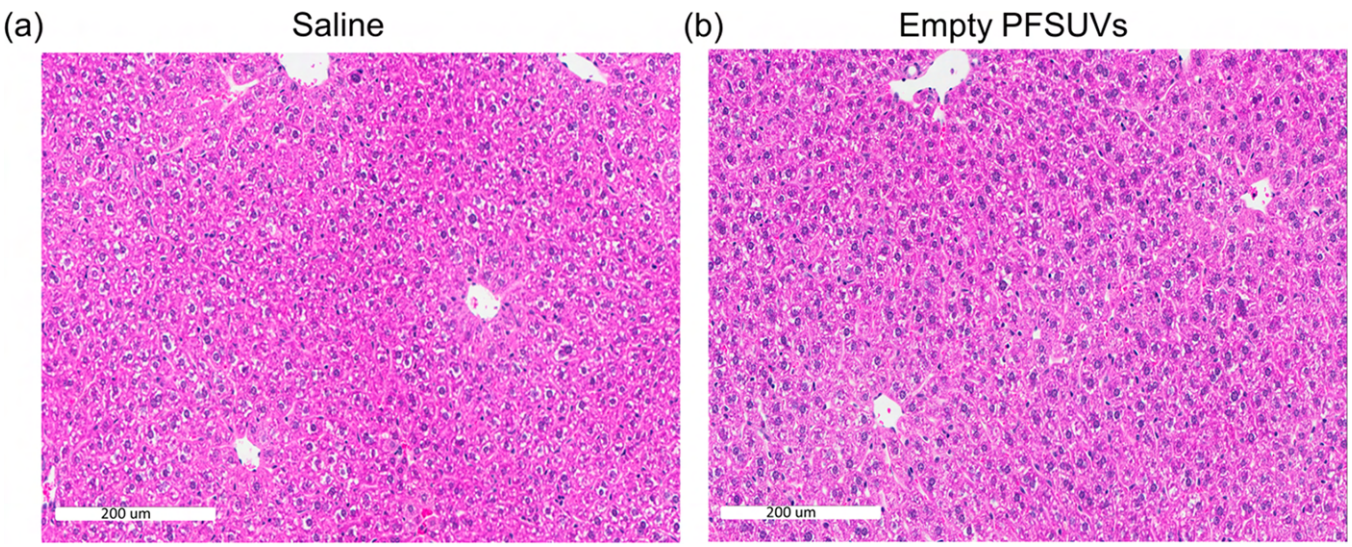

Figure 7. Representative images of hematoxylin and eosin-stained sections of mouse liver at 24 h after i.v. administration of (a) saline (b) empty PFSUVs at 100 mg total lipid/kg. Scale bar represents 200 μm.

https://doi.org/10.1021/acs.molpharmaceut.1c00520
Mol. Pharmaceutics 2022, 19, 1778−1785

Roland Böttger − *Faculty of Pharmaceutical Sciences, University of British Columbia, Vancouver, British Columbia V6T 1Z3, Canada*
Elham Rouhollahi − *Faculty of Pharmaceutical Sciences, University of British Columbia, Vancouver, British Columbia V6T 1Z3, Canada*
Pieter R. Cullis − *Department of Biochemistry and Molecular Biology and NanoMedicines Innovation Network (NMIN), University of British Columbia, Vancouver, British Columbia V6T 1Z3, Canada;* orcid.org/0000-0001-9586-2508
Dominik Witzigmann − *Department of Biochemistry and Molecular Biology and NanoMedicines Innovation Network (NMIN), University of British Columbia, Vancouver, British Columbia V6T 1Z3, Canada*

Complete contact information is available at: https://pubs.acs.org/10.1021/acs.molpharmaceut.1c00520

Funding

This work was supported by the Canadian Institutes of Health Research (CIHR, grant nos. PJT-148610 and PJT-168861), the Natural Science and Engineering Research Council in Canada (NSERC, grant no. RGPIN-2017-03787), the Canada Foundation for Innovation (CFI, grant no. 35816), and the Mitacs Accelerate grant (no. IT13402) sponsored by Mitacs and Precision Nanosystems Inc., Canada (grant no. 18004). S.D.L. received the Angiotech Professorship in Drug Delivery. N.A.F. received a full Ph.D. scholarship from King Abdulaziz City for Science and Technology (KACST) in Saudi Arabia. R.B. is supported by a postdoctoral fellowship from the German Research Foundation (DFG; grant no. 423802991). D.W. acknowledges the support by the Swiss National Science Foundation Postdoc Mobility Fellowship (no. 183923).

Notes

The authors declare no competing financial interest.

■ ACKNOWLEDGMENTS

We acknowledge Dr. Natalie Strynadka and Dr. Florian Rossmann from the UBC High Resolution Macromolecular Cryo-Electron Microscopy facility for supporting the cryo-TEM imaging. We thank Anitha Thomas and Samuel Clarke from Precision Nanosystems Inc. and Anne Nguyen for technical support in operating the NanoAssmeblr Benchtop. The table of contents graphic was created by author N.A.F. using biorender (https://biorender.com).

■ REFERENCES

(1) WHO, *World malaria report 2018*, WHO, 2019. http://www.who.int/malaria/publications/world-malaria-report-2018/en/ (accessed Oct 17, 2020).
(2) Ozarslan, N.; Robinson, J. F.; Gaw, S. L. Circulating Monocytes, Tissue Macrophages, and Malaria. *J. Trop Med.* **2019**, *2019*, 1.
(3) CDC. https://www.cdc.gov/dpdx/malaria/index.html (accessed Oct 17, 2020).
(4) Baird, J. K.; Hoffman, S. L. *Clin. Infect. Dis.* **2004**, *39*, 1336.
(5) Chen, V.; Daily, J. P. Tafenoquine: the new kid on the block. *Curr. Opin. Infect. Dis.* **2019**, *32*, 407−12.
(6) Duparc, S.; Beutler, E. Glucose-6-Phosphate Dehydrogenase Deficiency and Antimalarial Drug Development. *Am. J. Trop. Med. Hyg.* **2007**, *77*, 779−89.
(7) WHO, *Testing for G6PD deficiency for safe use of primaquine in radical cure of P. vivax and P. ovale (Policy brief)*, WHO, 2019.http://www.who.int/malaria/publications/atoz/g6pd-testing-pq-radical-cure-vivax/en/ (accessed Oct 17, 2020).
(8) Cappellini, M.; Fiorelli, G Glucose-6-Phosphate Dehydrogenase Deficiency and Antimalarial Drug Development. *Lancet* **2008**, *371*, 64−74.
(9) Zhang, W.; Bottger, R.; Qin, Z.; Kulkarni, J. A.; Vogler, J.; Cullis, P. R.; Li, S.-D. Glucose-6-Phosphate Dehydrogenase Deficiency and Antimalarial Drug Development. *Small* **2019**, *15*, 1901782.
(10) Chasis, J.; Schrier, S. Membrane deformability and the capacity for shape change in the erythrocyte. *Blood* **1989**, *74*, 2562−2568.
(11) Bowman, Z. S.; Morrow, J. D.; Jollow, D. J.; Mcmillan, D. C. *J. Pharmacol. Exp. Ther.* **2005**, *314*, 838−45.
(12) Vogler, J.; Bottger, R.; AL Fayez, N.; Zhang, W.; Qin, Z.; Hohenwarter, L.; Chao, P.-H.; Rouhollahi, E.; Bilal, N.; Chen, N.; Lee, B.; Chen, C.; Wilkinson, B.; Kieffer, T. J.; Kulkarni, J. A.; Cullis, P. R.; Witzigmann, D.; Li, S.-D. Altering the intra-liver distribution of phospholipid-free small unilamellar vesicles using temperature-dependent size-tunability. *J. Controlled Release* **2021**, *333*, 151−61.
(13) White, N. J.; Qiao, L. G.; Qi, G.; Luzzatto, L. Rationale for recommending a lower dose of primaquine as a Plasmodium falciparum gametocytocide in populations where G6PD deficiency is common. *Malar. J.* **2012**, *11*, 1−10.
(14) Geekiyanage, N. M.; Balanant, M. A.; Sauret, E.; Saha, S.; Flower, R.; Lim, C. T.; Gu, Y. A coarse-grained red blood cell membrane model to study stomatocyte-discocyte-echinocyte. *PLoS One* **2019**, *14*, e0215447.
(15) Eziefula, A. C.; Pett, H.; Grignard, L.; et al. *Antimicrob. Agents Chemother.* **2014**, *58*, 4971−3.
(16) Deuticke, B. Transformation and restoration of biconcave shape of human erythrocytes induced by amphiphilic agents and changes of ionic environment. *Biochim. Biophys. Acta, Biomembr.* **1968**, *163*, 494−500.
(17) CD-1 IGS Mice Nomenclature: Crl:CD1(ICR) Strain Origin. www.criver.com/info/rm (accessed March 5, 2021).